

Fast-ion Transport Induced by Edge Localized Modes¹

Haotian Chen^{1,2}

¹Southwestern Institute of Physics, China

²Center for Nonlinear Plasma Science, Italy

Oct. 27, 2024
Hangzhou

¹submitted to Nuclear Fusion, under review.

- 1 Background
- 2 Theoretical Model
- 3 Conclusion and Discussion

Background

Experimental Observations

Velocity space measurements of fast-ion losses reveal a population at **energies well above the main NBI injection energy during ELMs**²³.

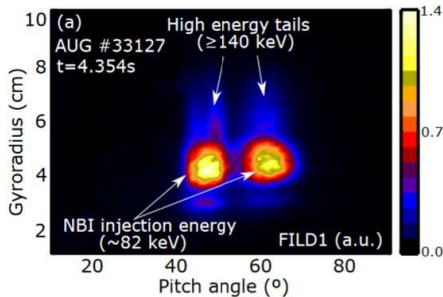


Figure 1: Velocity space measurement of fast-ion losses performed with FILD (fast-ion loss detector) during an ELM in AUG¹.

- Two populations can be observed at two main different pitch angles of $\pi/4$ (Q7, passing) and $\pi/3$ (Q8, trapped).
- NBI injects neutrals at **three different energies** $E_0 = 82\text{keV}$, $E_0/2$ and $E_0/3$.

²J. Galdon-Quiroga et al 2018 Phys. Rev. Lett. 121 025002

³J. Galdon-Quiroga et al 2019 Nucl. Fusion 59 066016

The observation of high-energy tail is **reproducible** and **well correlated** with the NBI heating and the occurrence of ELMs².

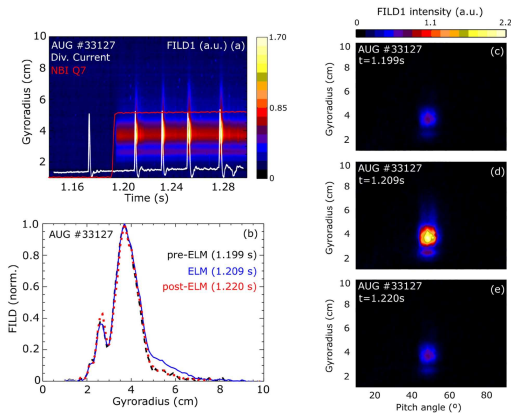


Figure 2: (a) Gyroradius profile evolution of the FILD signal at the relevant pitch angle in AUG shot 33127. The divertor current (white) is used as an ELM monitor. (b) Comparison between inter-ELM and intra-ELM gyroradii profiles obtained with FILD in shot 33127. (c), (d) and (e) show the complete velocity space measurement of FILD at these time points

- High-energy population **disappears** in the ELM suppressed regime.

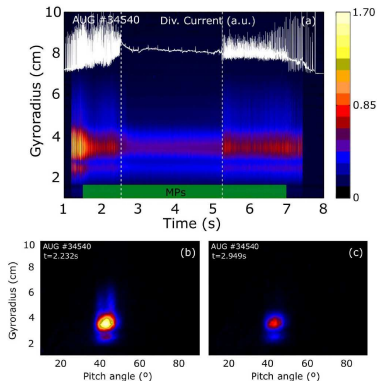


Figure 3: Gyroradius profile evolution of the FILD signal at the relevant pitch angle in AUG shot 34570, during which external MPs are applied (green box). The time window in which ELM suppression is achieved is indicated by two vertical dashed lines. The complete velocity space measured by FILD is shown at a time point before ELM suppression is achieved (b), and at a time point when ELMs are suppressed (c).

- High-energy population exhibits a **pitch angle structure** that depends on the **beam source** and q_{95} .
 - Trapped particles (Q8) correspond to a **weaker FILD signal**.
 - Multiple spikes are observed in AUG shot 34614 (**low q_{95}**), but **not** in 34615 (**high q_{95}**).

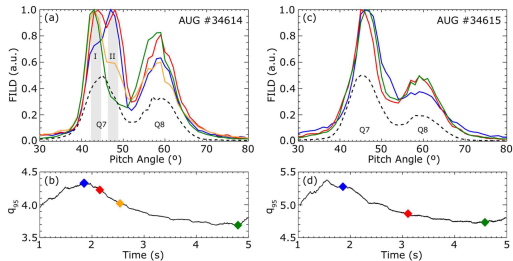


Figure 4: Pitch angle profile of the FILD signal for AUG shots 34614 and 34615, respectively.

- It was proposed^{1,2} that the high-energy population was **accelerated by the parallel electric field** emerging during ELMs, when magnetic reconnection is believed to take place⁴. However, this mechanism **cannot be an effective way to accelerate fast ions**, because:
 - it assumes a large amplitude parallel electric field with reference to previous simulation results, in which the parallel electric field strength depends on the magnitude of the artificial hyper-resistivity;
 - it accelerates charged particles only in the parallel direction, whereas the fast ion pitch angle does not change significantly in the experimental observations;
 - the parallel electric field, if present, will be highly localized around the thin current sheet, the width of which is much smaller than the fast ion gyroradius.
- The motivation of this work is thus to theoretically understand **where the high-energy fast-ion population measured during ELMs comes from**.

⁴A. W. Leonard 2014 Phys. Plasmas 21 090501

- We present a **gyrokinetic model** for the fast-ion 'acceleration'.
- Begin with the **gyrocenter Hamiltonian** in 5D phase space⁵:

$$H(\mathbf{X}, \mu, w, t, \tau) = \mu B + \frac{w^2}{2} + \frac{e}{m}(\langle \delta \phi \rangle - \frac{w}{c} \langle \delta A_{\parallel} \rangle + \frac{v_{\perp} \rho}{c} \langle \delta B_{\parallel} \rangle_*). \quad (1)$$

where the gyroaverage operator $\langle \delta B_{\parallel} \rangle_* = \frac{J_1(i\rho \nabla_{\perp})}{i\rho \nabla_{\perp}} \delta B_{\parallel}$ is related to the compressional component of the magnetic perturbation.

- Consistent with the gyrokinetic framework, we adopt the variables $\delta \phi$, $\delta \psi$ and δB_{\parallel} as well as the Coulomb gauge, where $-c \nabla_{\parallel} \delta \psi = \partial_t \delta A_{\parallel}$.
- Note that the **FLR effect** is retained for modes observed in experiments with $n \lesssim 10$.

⁵A. J. Brizard 1995 Phys. Plasmas 2 459

Gyrocenter Model

Fluctuations

- A single ELM crash can last typically $1ms$.
- Subdominant fluctuations with typical time scale on the order of $100\mu s$ are observed within a single ELM crash.
- Fast-ion slowing down time is $\sim 100ms$.

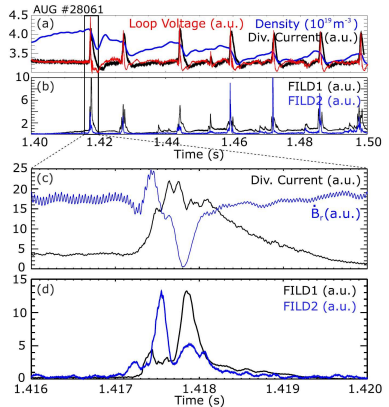


Figure 5: (a) Time traces of the edge electron density (in blue), the loop voltage (in red), and the divertor current (in black). (b) Time traces of two different FILD signals. (c) and (d) show an enlargement of an individual ELM²

- During the ELM crash a broad spread in frequency is generally measured in AUG but low frequencies $\omega \sim 10\text{kHz}$ are dominant, with $n \lesssim 5$ and $\delta B_{\perp}/B_0 \sim \mathcal{O}(10^{-3})$.
- The inter-ELM modes in a high frequency range $\omega \sim 100\text{kHz}$ appears in the linear and early nonlinear phases, with $n \sim 10$ and $\delta B_{\perp}/B_0 \sim \mathcal{O}(10^{-5} - 10^{-4})$.

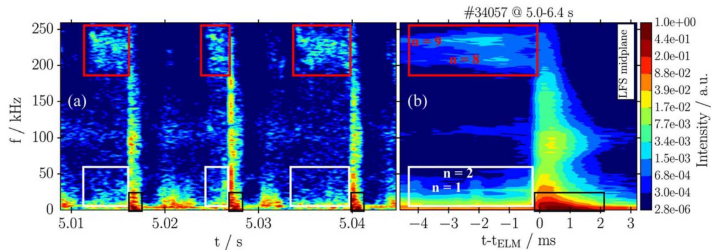


Figure 6: Typical spectrum during ELM crash in AUG⁶.

⁶A. F. Mink et al 2018 Plasma Phys. Control. Fusion 60 125011

- For the **core component**, the ideal MHD approximation remains valid, thus the **parallel electric field vanishes**, i.e., $\delta\phi = \delta\psi$.
- Due to the **perpendicular pressure balance in low- β limit**, δB_{\parallel} satisfies,

$$\frac{\delta B_{\parallel}}{B_0} \simeq \frac{4\pi en_i}{B_0^2} \frac{k_{\theta} c T_i}{e B_0 r_p} \frac{\delta\phi}{\omega}. \quad (2)$$

with $r_p^{-1} = |\partial_r \ln P|$.

- The **relative fluctuation levels** are estimated by the ordering parameter $\epsilon_B \equiv \delta B_{\perp}/B_0$:

$$\frac{e\delta\psi}{T_i} \sim \frac{2\omega}{k_{\perp} \rho_i k_{\parallel} v_i} \frac{\delta B_{\perp}}{B_0}, \quad \frac{\delta B_{\parallel}}{B_0} \sim \frac{\beta}{2r_p k_{\parallel}} \frac{\delta B_{\perp}}{B_0}. \quad (3)$$

With the **AUG parameters** of interest, one has $|\delta B_{\parallel}| \ll |\delta B_{\perp}|$.

- For **fast ions**, one can then estimate

$$\frac{w\delta A_{\parallel}}{c\delta\phi} \sim \frac{k_{\parallel} w}{\omega} \gg 1, \quad \frac{v_{\perp} \rho \delta B_{\parallel}}{w\delta A_{\parallel}} \sim \frac{v_{\perp} k_{\perp} \rho}{w} \frac{\delta B_{\parallel}}{\delta B_{\perp}} \ll 1. \quad (4)$$

Therefore, the **perpendicular magnetic perturbation dominates the perturbed Hamiltonian of fast ions**.

- From the Hamiltonian equation, the particle acceleration can be formally described by $\dot{H} = \partial_t \delta H$.
- This provides an order of magnitude estimate for the time required for the particle acceleration, $\Delta t \sim \Delta H / (\omega \delta H)$.
- Given that the observed energy variation is comparable to the unperturbed energy $\Delta H \sim H_0 = v_0^2/2$, one readily obtains

$$\Delta t \sim \frac{H_0}{\omega \delta H} \sim \frac{k_{\perp} \rho_0}{\omega} \frac{B_0}{\langle \delta B_{\perp} \rangle}. \quad (5)$$

- Substituting into parameters of low- n modes and inter-ELM modes, respectively, one can estimate the required time as

$$\Delta t_{low} \sim \mathcal{O}(10^3)/\omega_{low} \sim 1s, \quad \Delta t_{int} \sim \mathcal{O}(10^4 - 10^5)/\omega_{int} \sim 1 - 10s. \quad (6)$$

- Therefore, one concludes that both the inter-ELM modes and the dominant low- n modes cannot account for the observed fast ion 'acceleration' on $\sim 100\mu s$. Fast-ion is not accelerated by ELMs.
- This raises the issue of how to explain the observed fast ion 'acceleration' during ELMs.

- During the ELM crash, the system is characterized by **two time scales**, due to the existence of the ELM fluctuations.
- Consistent with the time-scale ordering in the present work, we adopt the **multi-scale perturbation method**, and assume that for **every bounce** the effect of **nonlinear dynamics is small** compared with the oscillations of the equilibrium particle trajectory. However, the cumulative effect of the nonlinear dynamics on **many bounce times** can be **large** and even connected with a secular process⁷.
- To incorporate the disparity between **unperturbed** and **perturbed** scales, we extend the number of time variables from t to t_0, t_1 , with

$$\frac{dt_1}{dt} \ll \frac{dt_0}{dt}. \quad (7)$$

⁷F. Zonca et al 2015 New J. Phys. 17 013052

An **arbitrary perturbation**, say δQ , can be **decomposed** into the **Lagrangian description**⁸ by introducing the **fast** (t_0) and **slow** (t_1) time scales,

$$\delta Q_n = e^{-in[\omega_\zeta t_0 + \partial_{P_\zeta} \omega_\zeta \int_0^{t_1} \delta P_\zeta dt' + \partial_E \omega_\zeta \int_0^{t_1} \delta E dt'] - in \int_0^{t_1} \delta \dot{\zeta} dt'} \sum_{m,l} e^{i(m\delta_c + l)[\omega_b t_0 + \partial_{P_\zeta} \omega_b \int_0^{t_1} \delta P_\zeta dt' + \partial_E \omega_b \int_0^{t_1} \delta E dt'] + im \int_0^{t_1} \delta \dot{\theta} dt'} c_{m,l}, \quad (8)$$

where we have introduced the unified notation ω_b for bounce and transit frequency of trapped and circulating particles, respectively; $\delta_c = 1$ ($\delta_c = 0$) for circulating (trapped) particles; and

$$c_{m,l}(E, \mu B_0, P_\zeta, t_1) = \oint \frac{\omega_b dt_0}{2\pi} e^{-il\omega_b t_0 - in\tilde{\zeta} + im\tilde{\theta}} A_n(\bar{r} + \underbrace{\tilde{r} + \int_0^{t_1} \delta \dot{r} dt'}_{\text{FDOW}}). \quad (9)$$

- Eq. (9) implies that, due to the **finite drift orbit width (FDOW)** effect, the **orbit-averaged fields for trapped particles** are typically smaller than those for circulating particles, leading to **weaker cross-field transport**.
- This is consistent with the experimental observation that **trapped particles has a weaker FILD signal**.

⁸F. Zonca et al 2015 New J. Phys. 17 013052

Wave-particle Resonance

Single island case

When we consider only the region near a **single phase-space island**, we can **neglect the nonlinear wave-particle resonance**, and introduce the **wave-particle phase** Θ as

$$\begin{aligned}\Theta = & n[\omega_\zeta t + \partial_{P_\zeta} \omega_\zeta \int^t dt \delta P_\zeta + \partial_E \omega_\zeta \int^t dt \delta E] \\ & - (\delta_c m + l)[\omega_b t + \partial_{P_\zeta} \omega_b \int^t dt \delta P_\zeta + \partial_E \omega_b \int^t dt \delta E] - \omega_n t,\end{aligned}\quad (10)$$

with ω_n being the complex mode frequency.

- From the Hamiltonian, we have

$$\delta \dot{P}_\zeta = -\partial_\zeta \delta H, \quad \delta \dot{E} = \partial_t \delta H, \quad (11)$$

therefore the wave-particle phase satisfies the nonlinear pendulum equation

$$\ddot{\Theta} + \omega_B^2 \sin \Theta = 0, \quad (12)$$

with the initial values $\Theta = \Theta_0$ and $\dot{\Theta} = \dot{\Theta}_0 = n\omega_\zeta - (\delta_c m + l)\omega_b - \omega_n (t=0)$.

- The **wave trapping frequency** is given by

$$\omega_B^2 = \delta H_{m,l} \{ n[n\partial_{P_\zeta} \omega_\zeta - (\delta_c m + l)\partial_{P_\zeta} \omega_b] + \omega_n [n\partial_E \omega_\zeta - (\delta_c m + l)\partial_E \omega_b] \}. \quad (13)$$

Wave-particle Resonance

Single island case

- Near a **single phase-space island**, the **maximum energy exchange** during the wave-particle interaction is

$$\delta E = \frac{2\omega_n H_{m,l}}{\omega_B}, \quad (14)$$

and the **maximum canonical momentum exchange**, meanwhile, is

$$\delta P_\zeta = \frac{2n H_{m,l}}{\omega_B}. \quad (15)$$

Here ω_B is the **wave trapping frequency**, and it is evident that $n\delta E - \omega_n \delta P_\zeta = 0$.

- The corresponding **radial displacement** δr can be expressed as

$$\delta r = \frac{2k_\theta H_{m,l}}{\Omega\omega_B}. \quad (16)$$

- Qualitatively, for both the **low- n modes** and **inter-ELM modes** during ELM crash with

$$\frac{\Delta E}{v_0^2} \frac{R_0}{\Delta r} = \frac{\omega_n R_0}{v_0 k_\theta \rho_0} \ll 1, \quad (17)$$

the **P_ζ exchange dominates the transport process**, as expected, where v_0 is the unperturbed fast ion velocity and $\rho_0 = v_0/\Omega_c$.

Wave-particle Resonance

Island overlapping condition

The **island overlapping condition** can be written in terms of the ratio between δr and the distance between mode rational surfaces

$$\frac{\delta r}{\Delta} \simeq 2\sqrt{k_{\theta}\rho_0} \sqrt{\frac{nq^2s}{\epsilon} \frac{J_0(k_{\perp}\rho_0)\delta B_{\perp}}{B_0}}. \quad (18)$$

- For the **low- n modes** with $n \simeq 2$, $q \simeq 4$, $s \simeq 4$, $\epsilon = 0.5/1.65$, $\rho_0/a \sim 0.1$, and $|\delta B_{\perp}/B_0| \sim \mathcal{O}(10^{-3})$, one has $k_{\theta}\rho \simeq 1$, and $\frac{\delta r}{\Delta} \simeq 1.42 > 1$.
- However, for the **inter-ELM modes** with $n \simeq 10$ and $|\delta B_{\perp}/B_0| \sim \mathcal{O}(10^{-4} - 10^{-5})$, one has $k_{\theta}\rho \simeq 5$ and $\frac{\delta r}{\Delta} \simeq 0.048 - 0.48 < 1$.
- Thus **only the islands due to low- n modes are overlapped**.
 - The **quasilinear theory** is best **applicable** when there may be waves that cause **orbit stochasticity due to mode overlap**.
- Noting also that $\delta r/\Delta$ is independent of parallel velocity, so the island **overlapping condition is determined by μB** .

The perturbed **nonadiabatic particle distribution** is given by

$$[\partial_t + \dot{\mathbf{X}} \cdot \nabla] \delta G = iQF_0 \delta H, \quad (19)$$

and the associated **radial particle flux** is

$$\Gamma_r(r, \mu, E) = \oint \frac{d\zeta}{2\pi} \oint \frac{d\theta}{2\pi} \delta \dot{r} \delta G. \quad (20)$$

Here, the **operator** Q is defined as

$$QF_0 \delta H = i \left[\frac{\partial F_0}{\partial E} \partial_t - \frac{\partial F_0}{\partial P_\zeta} \partial_\zeta \right] \delta \Phi, \quad (21)$$

and the **effective potential**

$$\delta \Phi = J_0 (\delta \phi - \delta \psi) + J_0 \frac{\omega_d \delta \psi}{\omega} + \frac{v_\perp J_1}{k_\perp c} \delta B_\parallel, \quad (22)$$

is due to three forces⁹: $\delta \phi - \delta \psi$ corresponds to the **parallel electric field**, which vanishes in the ideal MHD limit; $\frac{\omega_d \delta \psi}{\omega}$ arises from $\mathbf{v}_d \times \delta \mathbf{B}_\perp$; and the δB_\parallel term is **mirror force**.

⁹L. Chen 1999 J. Geophys. Res. 104 2421

- In the linear limit, the gyrokinetic equation can be solved as

$$\delta G = i\delta\Phi L^{-1} \left[\omega \frac{\partial F_0}{\partial E} + n \frac{\partial F_0}{\partial P_\zeta} \right]. \quad (23)$$

where the **propagator** $L = \omega - \mathbf{k} \cdot \dot{\mathbf{X}}$ accounts for the **wave-particle interaction**.

- Substituting the linear response to

$$\partial_t F_0 + \frac{\partial}{\partial P_\zeta} [\dot{P}_\zeta \delta G] + \frac{\partial}{\partial E} [\dot{E} \delta G] = 0, \quad (24)$$

yields the explicit **quasilinear transport equation**

$$\partial_t F_0 = \frac{\partial}{\partial \mathbf{J}} \cdot [\mathbf{D} \cdot \frac{\partial F_0}{\partial \mathbf{J}}]. \quad (25)$$

- The interaction of fast ions with turbulence is constrained to a **two-dimensional** $\mathbf{J} = (P_\zeta, E)$ **manifold** embedded in the full 6D phase space.

$$\partial_t F_0 - \frac{\partial}{\partial P_\zeta} [D_{P_\zeta P_\zeta} \frac{\partial F_0}{\partial P_\zeta}] - \frac{\partial}{\partial P_\zeta} [D_{P_\zeta E} \frac{\partial F_0}{\partial E}] - \frac{\partial}{\partial E} [D_{EP_\zeta} \frac{\partial F_0}{\partial P_\zeta}] - \frac{\partial}{\partial E} [D_{EE} \frac{\partial F_0}{\partial E}] = 0, \quad (26)$$

where the associated **transport coefficients** are defined as

$$D_{P_\zeta P_\zeta} = -\text{Im}[\frac{n^2 |\delta\Phi|^2}{L}], \quad (27)$$

$$D_{EE} = -\text{Im}[\frac{\omega^2 |\delta\Phi|^2}{L}], \quad (28)$$

and the off-diagonal terms

$$D_{P_\zeta E} = D_{EP_\zeta} = -\text{Im}[\frac{n\omega |\delta\Phi|^2}{L}]. \quad (29)$$

- In the **low-frequency ELM scale** ($|\omega| \ll k_\theta \rho_0 v_0 / R_0$), the diffusion will be constrained to a **1D manifold in P_ζ** .

- For **circulating particles**, as an example, the linear propagator is

$$L = \omega + (m - n\bar{q} + l)\omega_b - n\omega_d = \omega_n + (p - n\bar{q})\omega_b - n\omega_d + i\delta\omega, \quad (30)$$

with $p = m + l$, and $i\delta\omega$ denotes the **resonance broadening effect** (RBQ model here).

- Thus the **radial diffusion coefficient** becomes

$$D_{P_\zeta P_\zeta} = -\text{Im}\left[\sum_{n,p} \frac{n^2 |\delta\Phi_{n,p}|^2}{\omega_n + (p - n\bar{q})\omega_b - n\omega_d + i\delta\omega}\right]. \quad (31)$$

- The coefficient $D_{P_\zeta P_\zeta} \propto v_0^3$ due to $\delta\Phi_{n,p} \propto \omega_d$ and the summation over p , thus, in contrast to the microturbulence case ($D_{P_\zeta P_\zeta} \propto v_0^{-3}$)¹⁰, **high energy particles will be transported faster**, leading to **FILD signals seems like an acceleration process**.
- For typical AUG parameters, the **required time** for cross-field diffusion at edge is **on the order of $\Delta t \sim 100\mu\text{s}$** , consistent with experimental observations.

¹⁰W. Zhang, et al, Phys. Rev. Lett. 101, 095001 (2008).

The **resonance condition** for circulating and trapped particles are, respectively,

$$\omega + (m - n\bar{q} + l)\omega_b - n\omega_d = 0, \quad (32)$$

$$\omega + l\omega_b - n\omega_d = 0. \quad (33)$$

- Note that Eq. (23) depends on **poloidal mode number**, **spikes** correspond to **multiple phase space islands** for circulating particles.
- Unlike global AEs, **ELMs are localized in the edge region**, leading to a **restriction on the number of resonances**.
- A strong **decrease of n** (and thereby m) **with q** is observed in AUG⁵, resulting in variations of islands.

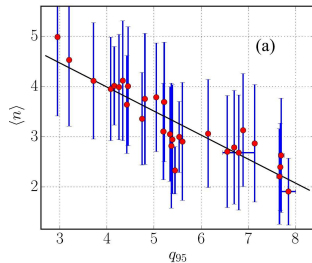
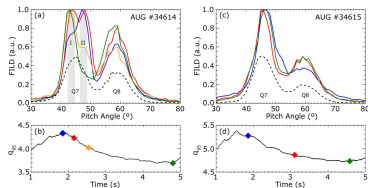


Figure 7: Averaged toroidal numbers $\langle n \rangle$ vs q_{95} during ELMs in AUG⁵.



A gyrokinetic model is developed to understand the ELM-induced fast-ion 'acceleration' observed in ASDEX Upgrade.

- The ELM crash cannot effectively accelerate fast ions, it induces an efficient radial transport of fast ions with $D_{P_\zeta P_\zeta} \propto v_0^3$, yielding a strong FILD signal in high energy tail.
- The transport is driven by the magnetic perturbation associated with low- n ELMs.
- Multiple spikes in pitch angle are due to multiple phase space islands for circulating particles.
- Theoretical predictions agree with the experimental observations:
 - Circulating particles are more easily transported, so the corresponding FILD signal is stronger. Due to the effects of finite drift orbit width and precessional resonance, the diffusivity of trapped particles is generally weaker ($D_{P_\zeta P_\zeta} \propto v_0^2$), resulting into a less pronounced FILD signal.
 - The required time for cross-field diffusion process is estimated as $\Delta t \sim 100\mu s$, consistent with experimental observations.